

## NUMERICAL SIMULATION OF THE CLOUD SEEDING OF A WARM BASE ILLINOIS CONVECTIVE CLOUD WITH AND WITHOUT ICE MULTIPLICATION ACTIVE

Harold D. Orville,<sup>1</sup> Fred J. Kopp,<sup>1</sup> Richard D. Farley,<sup>1</sup>  
and Robert R. Czys<sup>2</sup>

**Abstract.** Seeding simulations on a moderately vigorous, warm base, convective cloud produced a strong initial signal if ice multiplication was not active; no signal otherwise. Even though a strong effect was produced in the initial graupel field, no effect on the total rainfall was produced. The results lead to speculation about the effects of hygroscopic seeding of continental, cold base clouds. The large drops formed by the seeding could establish an ice multiplication process leading to cloud ice (and the resultant precipitating ice) at temperatures even higher than those due to ice-phase cloud seeding (such as silver iodide).

### 1. INTRODUCTION

This is another of our papers reporting on the results of numerical simulations of cloud seeding effects. This case treats the ice phase seeding of a moderately vigorous warm base convective cloud, similar to those active convective clouds observed on the Precipitation Augmentation for Crops Experiment (PACE) project conducted by the Illinois State Water Survey. Our only other cloud seeding simulation of a warm base convective cloud was reported on in an earlier WMA Journal paper (Orville *et al.*, 1989) and involved clouds from the Cooperative Huntsville Meteorological Experiment (COHMEX). An important difference in this current experiment is the modeling of ice multiplication in some of the simulations.

### 2. CLOUD DESCRIPTION

The atmospheric sounding from 23 June 1989 taken at the Willard Airport, Savoy, Illinois, was used as input to the cloud model. This day produced large convective clouds that were well observed by aircraft and radar. Clouds grew to 10 km and more. Cloud base temperatures were +15°C at a height of about 1.5 to 2.0 km. The sounding is shown in Fig. 1(a) and (b). Light winds were present as indicated in Fig. 1(b). Observations indicated a large number of cloud droplets and a broad droplet distribution. We used a number concentration of 972 droplets per cubic centimeter and a relative dispersion of 0.473 in the cloud model runs based on the observations.

Three experimental units were obtained on this day. Two received treatment with silver iodide and one with sand (a placebo case).

### 3. BRIEF CLOUD MODEL DESCRIPTION

The model used in this study is a two-dimensional, time-dependent cloud model (Orville and Kopp, 1977; Lin *et al.*, 1983) with bulk water microphysics and 200 m grid intervals over a 20 km by 20 km domain. Cloud seeding simulations employ techniques described in Hsie *et al.* (1980), Kopp *et al.* (1983), and Orville *et al.* (1984). The model is anelastic and uses a vorticity/stream function approach to obtain the velocity field. Chen and Orville (1980) provide additional information on the dynamic framework of the model.

The bulk water microphysical method is based on concepts suggested by Kessler (1969). Our model divides water and ice hydrometeors into five classes: cloud water, cloud ice, rain, snow, and high density precipitating ice (graupel/hail). Rain, snow, and graupel/hail, which are assumed to follow inverse exponential size distributions, possess appreciable terminal fall velocities. Cloud water and cloud ice have zero terminal velocities and thus travel with the air parcels. These five classes of hydrometeors interact with each other and water vapor through a variety of crude parameterizations of the physical processes of condensation/evaporation, collision/coalescence and collision/aggregation, accretion, freezing, melting, and deposition/

<sup>1</sup>Institute of Atmospheric Sciences, South Dakota School of Mines and Technology, 501 E. St. Joseph Street, Rapid City, South Dakota 57701-3995.

<sup>2</sup>Illinois State Water Survey, 2204 Griffith Drive, Champaign, Illinois 61820.

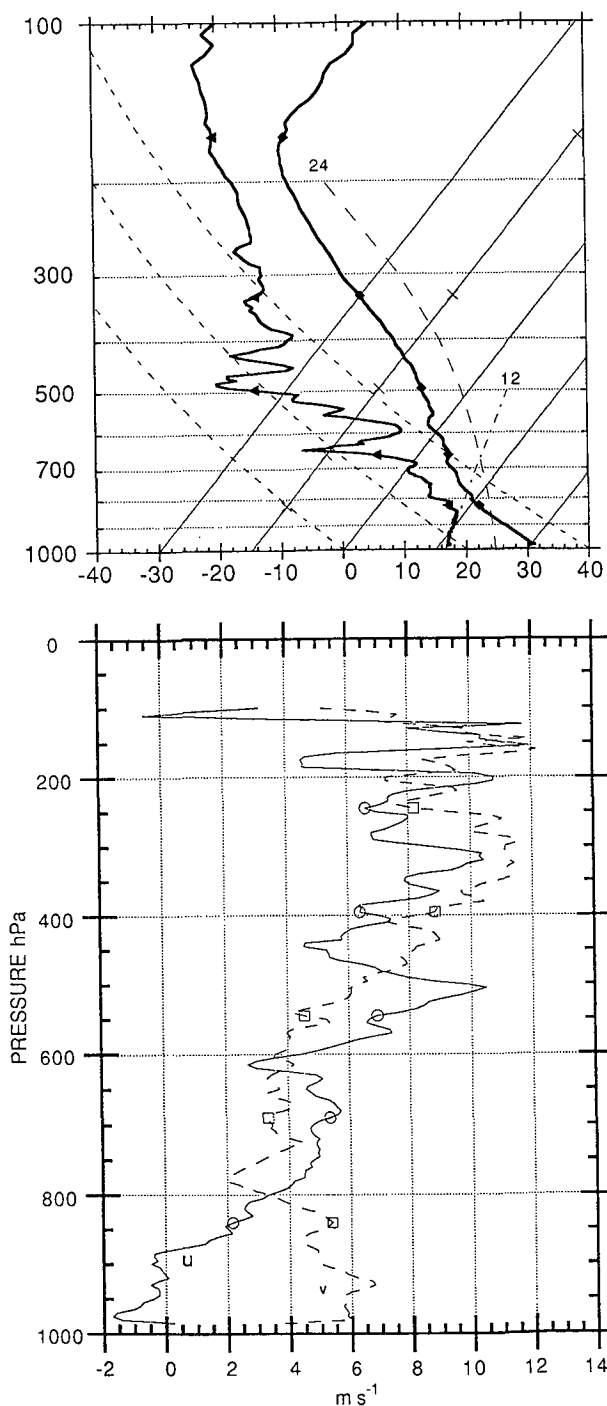


**Fig. 1:** The atmospheric sounding for 1252 CDT on 23 June 1989, Willard airport. a) Skew T-log p for temperature and moisture variables; b) winds U (west, positive), and V (south, positive).

sublimation. The microphysical processes and parameterizations employed in the bulk water model are discussed in detail by Wisner *et al.* (1972), Orville and Kopp (1977), and Lin *et al.* (1983).

The model was run with autoconversion (coalescence) activated and primary ice initiation at  $-20^{\circ}\text{C}$ . Freezing of rain drops begins as early as

$-5^{\circ}\text{C}$ . Cloud seeding was simulated assuming a drop of silver iodide flakes. The silver iodide creates ice crystals starting at  $-5^{\circ}\text{C}$ , but is more effective as the temperature lowers. The results from the seeding were compared with a run in which no seeding was simulated. In addition, two other runs were made with ice multiplication simulated, as described in Aleksić *et al.* (1989). One of the runs was seeded, one was unseeded. The important point to realize is that the ice multiplication routine generates cloud ice in the temperature region  $-3^{\circ}\text{C}$  to  $-8^{\circ}\text{C}$  if graupel is present. The efficiency of the process depends on the amount of cloud liquid in droplets larger than  $25\ \mu\text{m}$  in diameter.

#### 4. PRELIMINARY CLOUD MODEL RESULTS

##### 4.1 Normal Cases (No Ice Multiplication)

Figure 2 shows the development of the clouds in the unseeded and the seeded run, without ice multiplication active. A mean convergence value of  $5 \times 10^{-5}\ \text{s}^{-1}$  was superimposed in the lower atmosphere, no convergence in the middle atmosphere, and divergence of equal magnitude to the convergence in the upper atmosphere. This leads to upward vertical motions of a few cm/s in the domain and for a tendency for the thermals in the lower atmosphere to merge. The atmosphere becomes more unstable under convergence conditions in the lower atmosphere. There was ample evidence from the synoptic conditions for this day to use convergence in the model.

The figure and all of its panels cover the period from 57 min to 84 min. The solid line denotes the cloud outline (100% relative humidity); the dashed lines, the streamlines (units of  $\text{kg m}^{-2}\ \text{s}^{-1}$ ); the dots are rain mixing ratios; the S's are snow; and the asterisks are hail mixing ratios. Threshold values are  $1.0\ \text{g kg}^{-1}$  for the rain and hail and  $0.5\ \text{g kg}^{-1}$  for the snow. The left column panels are for the unseeded case; the right column ones for the seeded case. The first panel for the seeded case at 57 min shows the initial distribution of the silver iodide, an assumed drop of flakes. The quantity of AgI is  $100\ \text{g/km}$  in the y-direction.

Precipitation in the unseeded case forms primarily and initially from the coalescence of cloud water to rain water. An extensive rain field is obvious at 60 min of simulated real time. A small amount of graupel/hail had formed at 57 min, but the quantity was too small to show up on these graphs. Snow and graupel appear by 63 min as the cloud top passes the  $-20^{\circ}\text{C}$  level (7 km,  $0^{\circ}\text{C}$  is at about 4 km and  $-10^{\circ}\text{C}$  at 5.6 km). The snow field is above the rain field, but some graupel/hail is falling through the rain. Precipitation reaches the ground at about 69 min, and a substantial microburst is produced thereafter (about  $25\ \text{m s}^{-1}$  horizontal wind speed

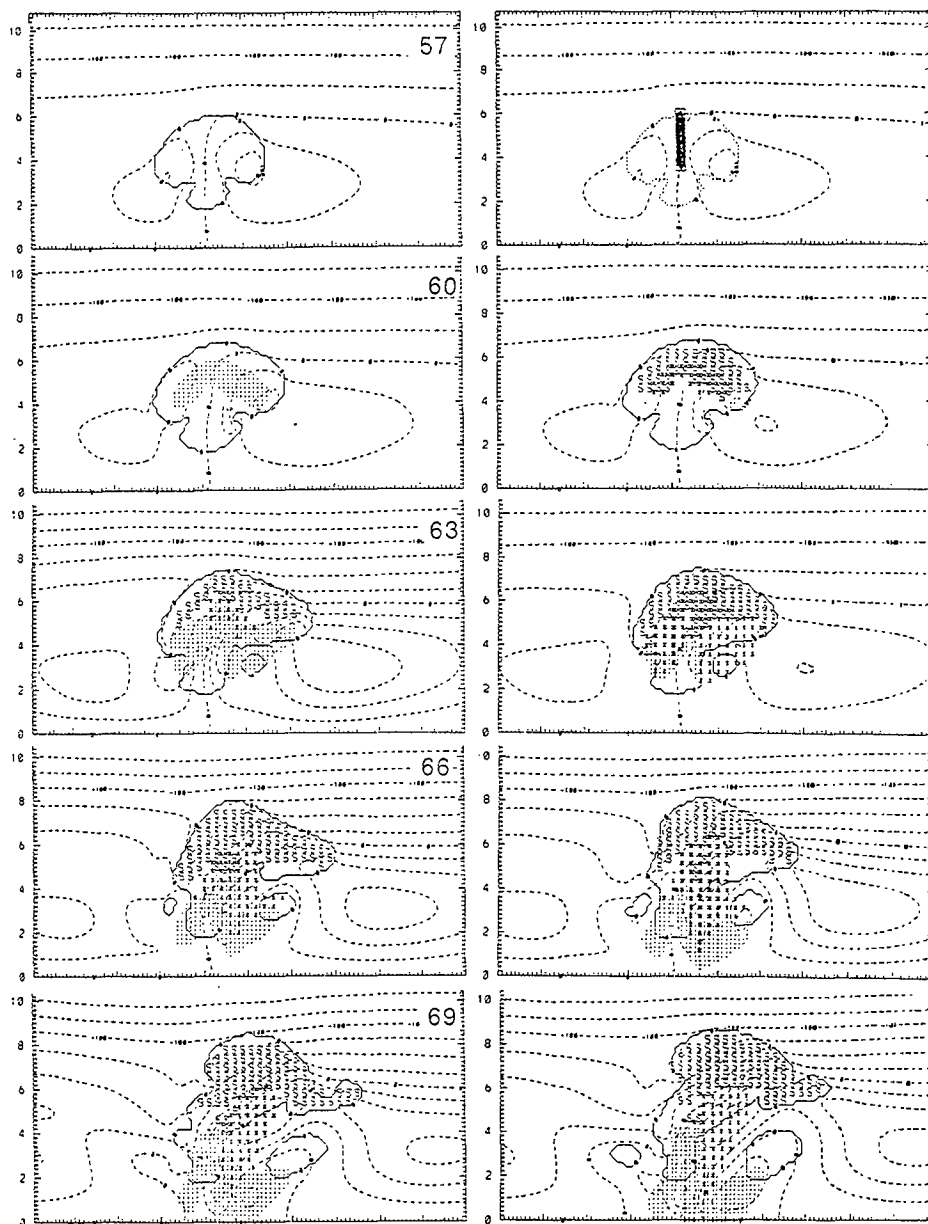


Fig. 2: Cloud history for the unseeded (left column) and seeded (right column) cases. The model domain covers 20 km in the horizontal and 20 km in the vertical, but the top is cut off at 10 km in this depiction. Dashed lines are streamlines; solid lines outline the cloud; dots indicate regions of rain greater than  $1 \text{ g kg}^{-1}$ ; S is snow greater than  $0.5 \text{ g kg}^{-1}$ ; \* is hail greater than  $1 \text{ g kg}^{-1}$ . At 57 min, no precipitation is yet visible in the unseeded case; and in the seeded case, the solid vertical bar outlines the initial pattern of the seeding material that is in the cloud at this time.

difference at the ground). The cell has produced most of its precipitation fallout by 81 min. Nearly 22 mm peak depth of rain is produced. Remnants of the cell persist until 93 min and later.

Ice precipitation in the seeded case begins much differently than in the unseeded case. The panel at 60 min shows the upper part of the cloud almost completely filled with snow and graupel/hail. This has happened because of the interaction of the artificially produced ice crystals with the rain. Small amounts of rain interacting with the ice crystals produce snow in the model; large values

of rain content interacting with ice crystals produce graupel/hail in the model cloud. Small areas of rain are present at the melting level on either side of the cloud at about the 4 km level. The precipitation develops rapidly and falls towards the ground, reaching the ground a minute or two before the rain in the unseeded case. At later times, the seeded case produces a very light shower from a small cloud in the center of the domain. As might be expected, the radar reflectivity pattern shows the earlier development of graupel/hail also. A difference of 10 dB exists at the early stages of precipitation development.

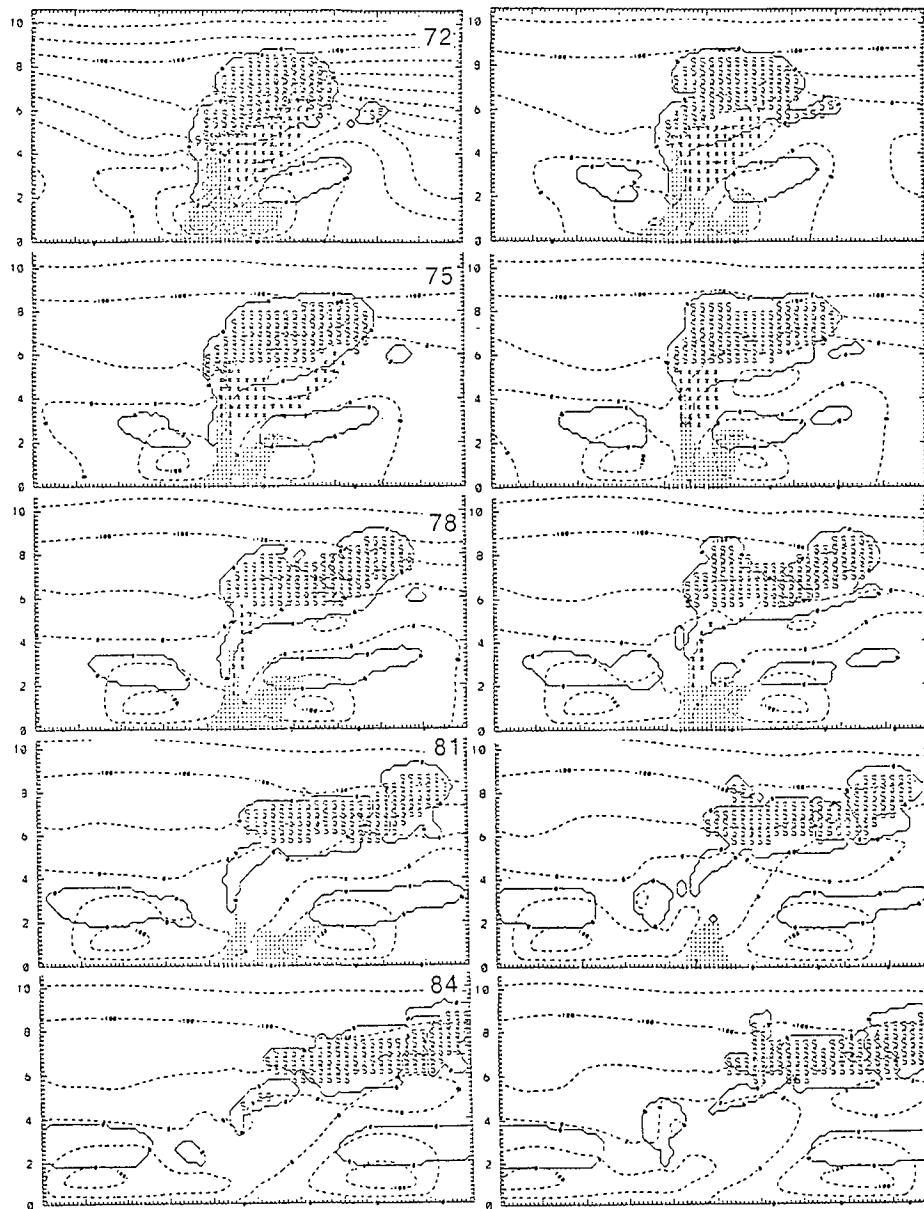


Fig. 2: (continued).

The total amount of precipitation accumulated on the ground is nearly identical in the two cases, although the seeded case produced its precipitation slightly sooner (see Figs. 3, 4, and 5). Even though the supercooled rain was transformed to precipitating ice rapidly, no strong dynamic effect of the seeding was detected. One to two  $\text{g kg}^{-1}$  of rain were rapidly transformed to ice. The extra heating ( $0.5^\circ\text{C}$ ) was evident in the temperature graphs, but was not enough to alter the dynamics of the cloud significantly. That may only have occurred if a mid-level capping inversion had been present.

Figures 3 and 4 show the accumulated rain and graupel/hail on the ground versus time. About

65 Ktons/ $\text{km}^2$  of precipitation are produced; 98% of it is rain. Figure 5 shows the distribution of the rain on the ground in the unseeded and seeded runs. Slight redistribution of the rain is evident.

Figure 6 indicates some of the main differences in the production of precipitation in the two cases. The unseeded case shows the formation of rain starting at about 57 minutes after model start-up (simulated real time). The ice precipitation begins at 61 minutes, graupel showing up a little before the snow. This is caused by the formation of graupel through the freezing of rain, while the initial formation of snow awaits the initiation of cloud ice.

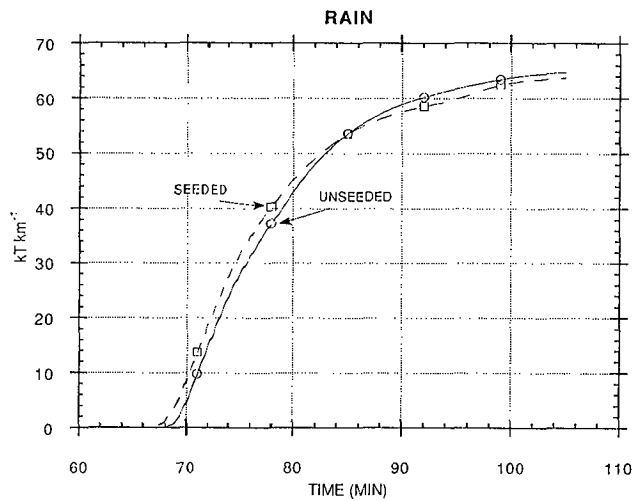


**Fig. 3:** Rain in kilotons per kilometer on the ground simulated in the model. The per kilometer refers to the unresolved third dimension (all dependent variables are assumed constant in the y-direction).

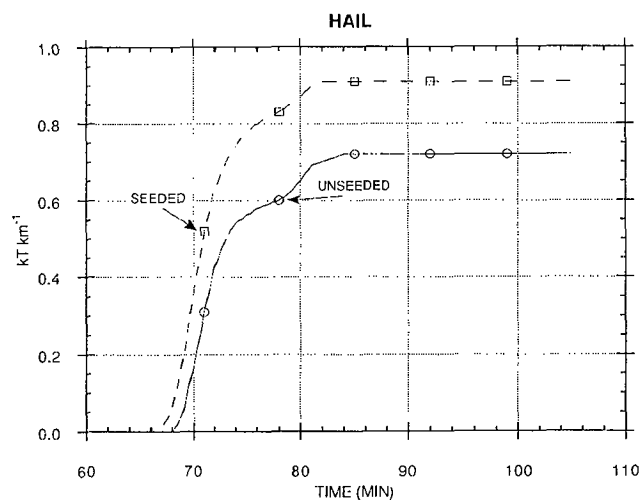


**Fig. 4:** Hail in kilotons per kilometer on the ground (as in Fig. 3).

The picture is different for the seeded case. Rain begins as before via coalescence, but the AgI seeding at 57 minutes produces artificial ice crystals which then interact with the rain to form snow and graupel. The graupel/hail peaks at about 64 minutes, about 2 minutes earlier than in the unseeded case. The graupel/hail falls into the melting layer after 63 minutes forming rain which, after 66 minutes, mimics the production of rain in the unseeded case.

These results indicate that the initial rain formation in the unseeded case is from coalescence of cloud water to rain and then growth of the rain by collection of the cloud. This growth peaks at about

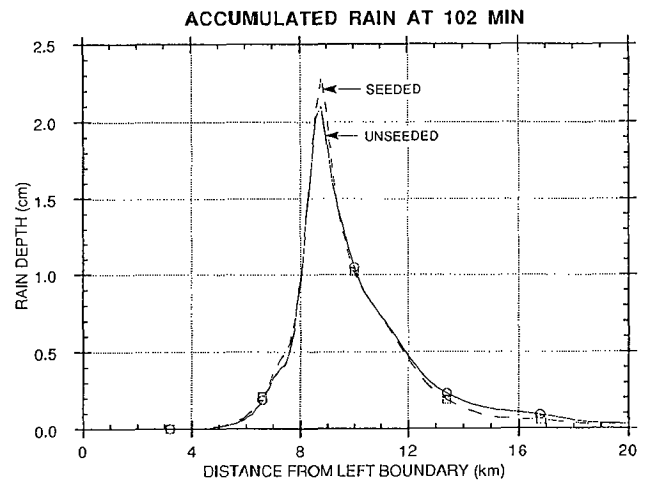


**Fig. 5:** Rainfall on the ground as measured by a rain gage at 102 minutes.

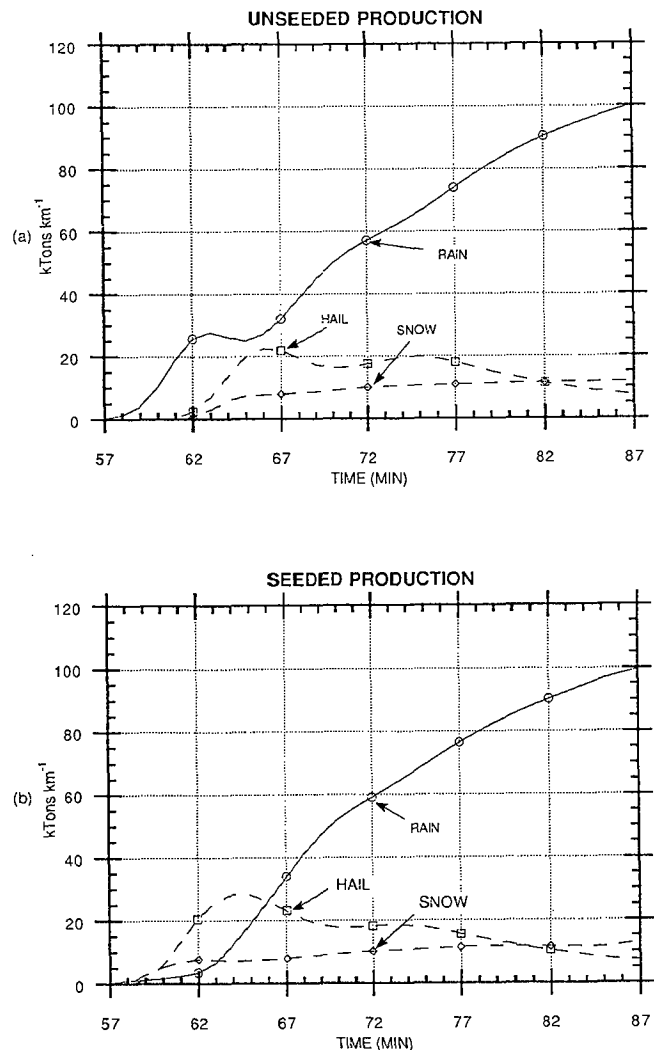


**Fig. 6:** Production of precipitation in kilotons per kilometer (as in Fig. 3). The curves for rain, hail, and snow are given vs. time. Note that the rain is converted to hail in the seeded case initially.

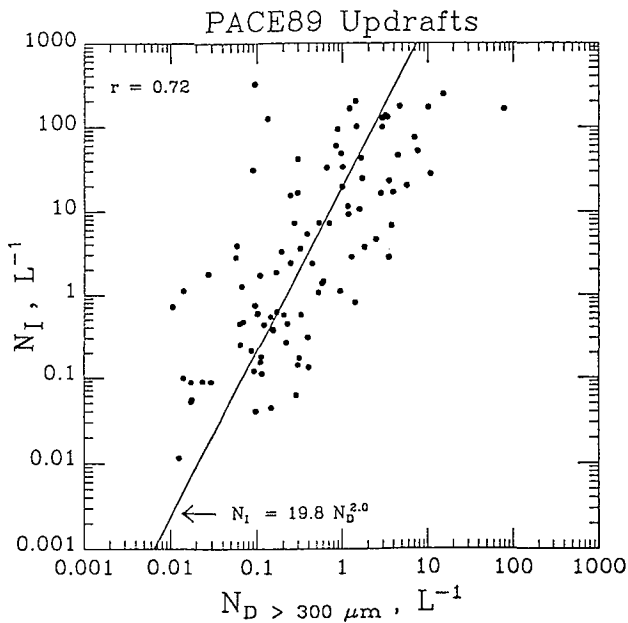


Fig. 7: Number of ice particles vs. number of drops > 300  $\mu\text{m}$ .

62 minutes and then begins to drop off. The surge in the rain production starting at 66 minutes is due to the fallout and melt of graupel and is common to both unseeded and seeded cases.

#### 4.2 Ice Multiplication Active

Figure 7, provided to us by the ISWS, indicates that the presence of ice in the updrafts of the PACE clouds depends in part on the presence of large drops, drops with diameters greater than 300  $\mu\text{m}$ . Consequently, we ran two cases simulating the physics of the Hallett-Mossop ice process, as parameterized by Aleksić *et al.* (1989). Figure 8 presents the main result. Ice multiplication in the unseeded case masks any effect of cloud seeding

in this case. This is due to the presence of large drops (rain) in the updrafts of the cloud, the freezing of some of the rain to produce some graupel, and the interaction of the graupel with the cloud water droplets (numerous and with a broad relative dispersion). This produces cloud ice at a relatively warm temperature ( $-5^\circ\text{C}$ ) and leads to snow and further graupel production. The seeded case has a nearly undetectable effect; one additional snow symbol appears in the cloud in this figure.

Figure 9 shows the formation of cloud ice in (1) the unseeded case - no ice multiplication; (2) the seeded case with ice multiplication; and (3) the unseeded case with ice multiplication active. There is nearly a one kilometer height difference between the cases, and a significant difference in cloud temperature at the height where the initial cloud ice appears. The seeded case with ice multiplication shows up intermediate to the two other cases because of its greater mixing ratio values (nearly three orders of magnitude greater). These results would indicate that no differences would be found in the precipitation production of the seeded and unseeded cases with ice multiplication active, which is indeed what resulted.

#### 5. SUMMARY AND SPECULATION

The numerical simulation of this relatively vigorous convective cloud has resulted in some added insight into the complexities of the seeding process and its effects on clouds -- at least numerical clouds. The seeding test on the cloud without an ice multiplication process active led to some very clear seeding signals near the time of seeding, but not in the final precipitation on the ground. The signals were rapid transformation of the rain to ice precipitation and a rapid increase in the radar reflectivity. Very slight changes in the vertical velocity were evident, and a change in the cloud temperature

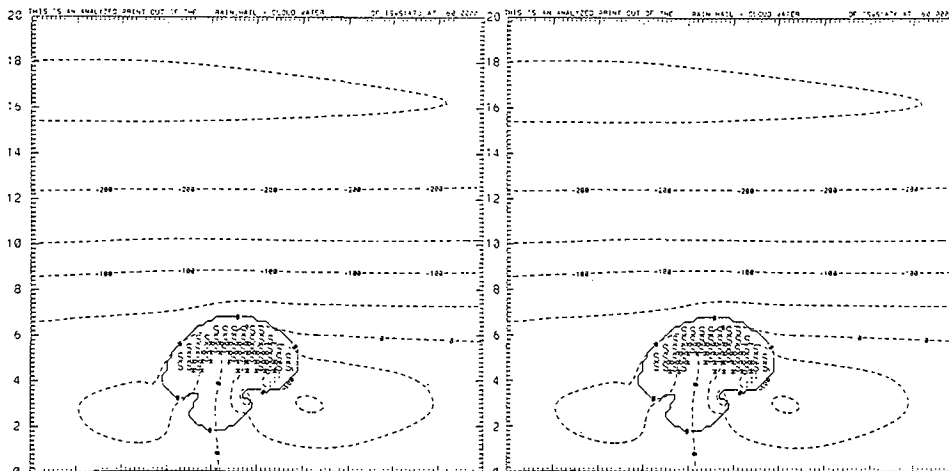
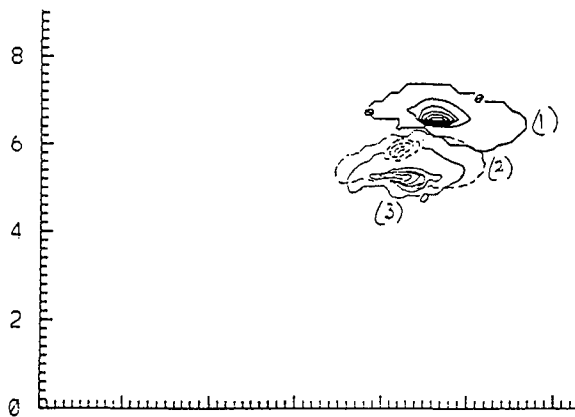


Fig. 8: As in Fig. 2, except for the ice multiplication case at 60 min. Left panel is for the unseeded case; right is seeded.



**Fig. 9:** Cloud ice patterns at 57 min showing the initial location of significant amounts of cloud ice in the (1) unseeded/unactivated ice multiplication case; (2) the seeded/activated ice multiplication case (dashed line); and (3) the unseeded/activated ice multiplication case. Note that only the lower left portion of the grid is shown in this figure.

was positive in the seeded cloud. The results with ice multiplication activated in the model code showed a nearly complete masking of the seeding effect, and no significant differences between the seeded and unseeded cloud at any time.

These results are different from those of Orville *et al.* (1989) where a very vigorous seeded cloud showed less rain than its unseeded counterpart, while a moderate shower cloud (seeded) showed a positive effect from the seeding. However, no ice multiplication was simulated in the earlier study.

A less vigorous warm base convective cloud may show some effects of ice phase seeding, even with an ice multiplication process active. Further studies are certainly warranted, and another case from the PACE data set is scheduled for study.

These results lead to speculation regarding the hygroscopic seeding of continental type cold base convective clouds. Such seeding may lead to early appearance of ice in the cloud. The results shown above indicate that cloud ice appears lowest in the cloud when ice multiplication is active. The hygroscopic seeding of a continental cold base cloud could lead to the formation of large drops which could then freeze to form graupel. This could activate an ice multiplication process in limited regions of the cloud which would then initiate ice in a relatively warm portion of the cloud. We plan to test this concept on some of the numerical simulations that we have conducted previously.

These results are model dependent and have been obtained on one case from the PACE data set.

The bulk water microphysics develop precipitation too soon once a precipitation species is formed. The concepts evolving from these studies should be tested in more detailed microphysical models, whenever possible.

**Acknowledgments.** We thank Joie Robinson and Carol Hirsch for helping in the preparation of this paper.

Support of the National Science Foundation under Grant No. ATM-9206919 is gratefully acknowledged. This research was supported by the University of Illinois at Urbana-Champaign under Subcontract No. 92-166 which is a part of the National Oceanic and Atmospheric Administration's Federal/State Cooperative Program under Contract No. NA 27RA0173-01.

## REFERENCES

- Aleksić, N. M., R. D. Farley and H. D. Orville, 1989: A numerical cloud model study of the Hallett-Mossop ice multiplication process in strong convection. *Atmos. Res.*, **23**, 1-30.
- Chen, C-H., and H. D. Orville, 1980: Effects of mesoscale convergence on cloud convection. *J. Appl. Meteor.*, **19**, 256-274.
- Hsie, E-Y., R. D. Farley and H. D. Orville, 1980: Numerical simulation of ice-phase convective cloud seeding. *J. Appl. Meteor.*, **19**, 950-977.
- Kessler, E., 1969: On the distribution and continuity of water substance in atmospheric circulations. *Meteor. Monogr.*, **32**. 84 pp.
- Kopp, F. J., H. D. Orville, R. D. Farley and J. H. Hirsch, 1983: Numerical simulation of dry ice seeding experiments. *J. Climate Appl. Meteor.*, **22**, 1542-1556.
- Lin, Y-L., R. D. Farley and H. D. Orville, 1983: Bulk parameterization of the snow field in a cloud model. *J. Climate Appl. Meteor.*, **22**, 1065-1092.
- Orville, H. D., and F. J. Kopp, 1977: Numerical simulation of the life history of a hailstorm. *J. Atmos. Sci.*, **34**, 1596-1618. [Reply: *J. Atmos. Sci.*, **35**, 1554-1555]
- Orville, H. D., F. J. Kopp, R. D. Farley and R. B. Hoffman, 1989: The numerical modeling of ice-phase cloud seeding effects in a warm-base cloud: Preliminary results. *J. Wea. Modif.*, **21**, 4-8.
- Orville, H. D., R. D. Farley and J. H. Hirsch, 1984: Some surprising results from simulated seeding of stratiform-type clouds. *J. Climate Appl. Meteor.*, **23**, 1585-1600.
- Wisner, C. E., H. D. Orville and C. G. Myers, 1972: A numerical model of a hail-bearing cloud. *J. Atmos. Sci.*, **29**, 1160-1181.